BRCORP
TECHNOLOGY | INNOVATION | INDUSTRY

International Journal of
Advanced Structures and Geotechnical Engineering
ISSN 2319-5347, Vol. 04, No. 02, April 2015

Macro and Micro Responses of Granular Materials under Plane Strain Compression by 3D DEM

MD. MAHMUD SAZZAD[1*], SAYERA KAWSARI[1], RIPON KUMER SHAHA[2], MD. SHEHABUL ISLAM[3]
[1]*Department of Civil Engineering, Rajshahi University of Engineering & Technology, Bangladesh*
[2]*Department of Civil Engineering, Lakshmipur Polytechnic Institute, Lakshmipur, Bangladesh*
[3]*Kwun Tong Apparels Ltd.,Adamjee Export Processing Zone, Bangladesh*
Email:mmsruet@gmail.com, riponce07@gmail.com, shihab_ce@yahoo.com

Abstract: This study presents the macro- and micro-mechanical responses of granular materials under plane strain compression (PSC) using the discrete element method (DEM). Three cubical shaped samples having different void ratios were numerically prepared using eleven different sizes of spheres, the diameter of which ranges from 3 to 4 mm. The spheres were randomly placed in a cubical shaped sample in such a way that no sphere should touch the other and later, compressed isotropically to 100 KPa using the periodic boundaries. The numerical samples prepared in this way were subjected to shear deformation under PSC. It is noted that the simulated stress-strain-dilative behaviors are in good agreement with the experimental studies under PSC for different void ratios. The evolution of a non-dimensional parameter b $[=(\sigma_2-\sigma_3)/(\sigma_1-\sigma_3)]$ with axial strain for different void ratios is reported as well. The micro-responses depict that their evolution depends on the void ratio and loading conditions of the simulations. The fabric measure evolve during shear deformation is presented in details and it is noted that the evolution of fabric measure has an excellent similarity to that of the stress ratio in PSC. A relationship between the macro stress ratio and the micro-parameter is established as well.

Keywords: *Plane strain compression, Micro-parameters, Discrete element method, b-value, Fabric*

1. Introduction:

Plane strain compression (PSC) tests are necessary to model, for example, the behavior of long embankments for roads or railways, where the strain parallel to the longitudinal axis of the embankment is almost zero. Consequently, the investigation of the macro- and micro-behaviors of granular materials for PSC is significant. A number of experimental studies have been devoted in the literature to investigate the behavior of granular materials under PSC (e.g., Cornforth, 1964; Lee, 1970; Tatsuoka et al., 1986; Peters et al., 1988; Alshibli et al., 2003; Yasin and Tatsuoka, 2006; Alshibli and Akbas, 2007; Tejchman and Wu, 2010). In the experimental studies, the macro mechanical responses such as stress, strain, volumetric strain, dilatancy index, etc. can be observed easily; however, it is hardly possible to explore the micro-behavior of granular materials such as the coordination number, sliding contact fraction, evolution of fabric etc. at particle-scale in laboratory based experimental studies for PSC test under different void ratios because of the limitations of the current experimental facilities. It should be emphasized that the knowledge of micro-characteristics is important to explain the macroscopic phenomena from the micro-mechanical point of view and to develop physically sound and micro-mechanical based continuum models.

This inherent limitation of experiments can be avoided using the numerical approaches such as the DEM (Cundall and Strack, 1979), which can model the discrete behavior of granular materials and provide inside into the micro features of the particulate system. Using DEM, the evolution of micro variables can be studied and micro data can be extracted at any stage of simulation. However, there are inadequate studies reported in the literature that considered PSC in three-dimensional (3D) DEM for different void ratios to explore the micro-mechanical responses of granular materials comprehensively. For example, Ng (2004) considered several stress paths with different sample preparation methods to report the macro- and micro-responses of granular materials including PSC by 3D DEM. However, the evolution of a non-dimensional parameter b defined as $b=(\sigma_2-\sigma_3)/(\sigma_1-\sigma_3)$, where σ_1, σ_2 and σ_3 are the major, intermediate and minor principal stresses, respectively (along x_1 -, x_2 - and x_3 - direction) for different void ratios under PSC is not reported and micro-mechanical responses are not studied sufficiently in earlier studies. Consequently, in the present study, the evolution of b value for different void ratios under PSC is reported and a comprehensive study of different micro-behaviors of granular materials under PSC by 3D DEM is presented. A linkage between the micro- and macro-parameters is established as well.

2. About DEM:

Discrete element method (DEM) is one of the most popular discrete approaches that describe the internal behavior of granular materials such as sand in a particulate system. The method was first introduced by Cundall (1971) for rock mass problem and later,

extended to soil (Cundall and Strack, 1979). DEM has been proved to be a useful tool to understand the physical processes such as the rotation, acceleration, contact force etc. of each particle involved in the model. DEM has been used successfully in different disciplines of science and engineering. The major advantage of DEM is that the micro data can be monitored and extracted at any stage of simulation for the post process and analysis. The fundamental idea of DEM is simple. Each particle is modeled as an element which can make and break contact with other elements included in the model. The DEM uses an explicit finite-difference scheme in which the calculation cycle includes the application of Newton's second law of motion and a force displacement law. The accelerations of particles are calculated using the following formula:

$$m\ddot{x}_i = \sum F_i \qquad i = 1,3 \qquad (1)$$

$$I\ddot{\theta} = \sum M \qquad (2)$$

where, F_i are the force components on each particle; M is the moment; m is the mass; I is the moment of inertia; $\ddot{x}_i$ are the components of translational acceleration and $\ddot{\theta}$ is the rotational acceleration of the particle.

3. About the Program Code OVAL:

In this study, computer code OVAL (Kuhn, 2006) is used. OVAL is written in FORTRAN and can run both in windows and Linux platform. Both 2D and 3D simulation is possible using OVAL. The effectiveness of OVAL has already been recognized (Kuhn, 1999; Kuhn, 2005). In OVAL, a simple contact force mechanism consisting of linear springs in normal and tangential directions and a frictional slider are included. The coefficient of viscosity for translational and rotational body damping used in this program represents a fraction of the critical damping $2\sqrt{mk_n}$ and $2r\sqrt{Ik_t}$, where r, k_n and k_t denotes the radius, normal and tangential contact stiffness of the particle, respectively.

4. Preparation of Numerical Sample:

In the present simulation, 8000 spheres (diameter 3 to 4 mm) consisting of 11 different sizes were randomly generated in a cube. This initially generated sparse sample was consolidated to 100 kPa using the periodic boundaries in several steps by assigning the coefficient of inter-particle friction coefficient of 0.0, 0.2 and 0.4 for the first, second and third samples, respectively. However, the desired inter-particle friction coefficient (i.e., 0.5) was used during shear. The characteristics of the three isotropically compressed samples S1, S2 and S3 are presented in Table 1. Coordination number in Table 1 is defined as twice the total number of contacts between particles divided by the total number of particles used in the simulation.

Table 1: Characteristics of the three isotropically compressed samples

Sample Designation	Void Ratio	Coordination Number
S1	0.58	5.9
S2	0.68	4.8
S3	0.73	4.2

5. Numerical Experiments:

Three isotropically compressed samples having different void ratios were used for the numerical simulations of PSC test. Simulations of PSC test were carried out by applying a very small strain increment of 0.00002% vertically downward in x_1-direction and keeping the strain in x_2- direction zero (i.e., $d\varepsilon_2 = 0$) while maintaining the stress in x_3-direction constant (100 kPa). The simulation condition of PSC test with reference axes is depicted in Figure 1. The DEM parameters used in the numerical simulation are shown in Table 2.

6. Numerical Result

6.1 Macro-mechanical responses:

The simulated stress-strain behavior for PSC test having different void ratios of the samples is depicted in Figure 2. It is noted that the stress ratio σ_1/σ_3 for sample S1 (void ratio 0.58) attains a peak state at small strain range followed by a huge strain softening, whereas for sample S3 (void ratio 0.73), σ_1/σ_3 gradually increases

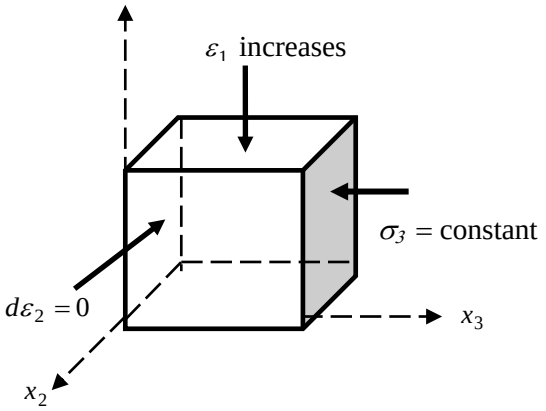

Figure 1: A cube element with reference axes and simulation conditions

Table 2: DEM parameters used in the numerical simulation

DEM parameters	Value
Normal contact stiffness (N/m)	1×10^6
Tangential contact stiffness (N/m)	1×10^6
Mass density (Kg/m^3)	2600
Increment of time step (s)	1×10^{-6}
Inter-particle friction coefficient	0.50
Damping coefficients	0.05

with axial strain ε_1. It is observed that σ_1/σ_3 merges each other at a large axial strain (at ε_1=10%) regardless of the void ratio of the samples. The behavior depicted in Figure 2 is a typical behavior for dense, medium and loose sand observed in the experimental studies under PSC. This numerical result is consistent with the experimental observation (e.g., Cornforth, 1964; Alshibli et al., 2003) which ensures the qualitative validation of the simulated stress-strain response. Similar tendency is also noticed in Figure 3 for the relationship between stress ratio σ_2/σ_3 and ε_1. Note that, the value of σ_2/σ_3 is small compared to σ_1/σ_3 at the same strain level.

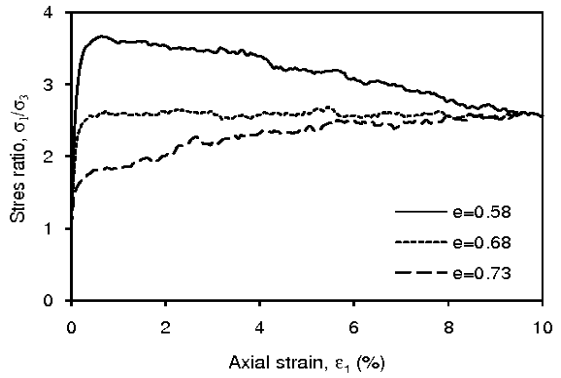

Figure 2: Relationship between stress ratio σ_1/σ_3 and axial strain ε_1

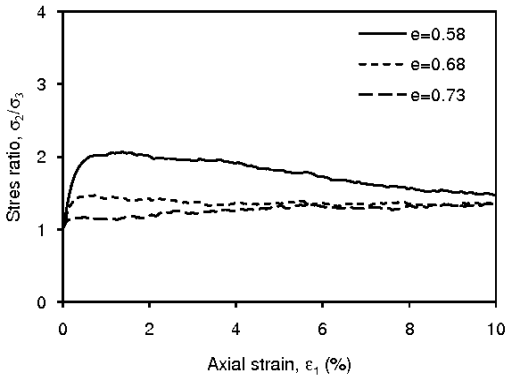

Figure 3: Relationship between stress ratio σ_2/σ_3 and axial strain ε_1

Figure 4 depicts the relationship between the volumetric strain ε_v and axial strain ε_1. The volumetric strain is defined here as $\varepsilon_v = \varepsilon_1 + \varepsilon_2 + \varepsilon_3$, where ε_1, ε_2 and ε_3 are the strains in x_1-, x_2- and x_3- direction, respectively. A positive value ε_v in Figure 4 represents compression, while a negative value represents dilation. From Figure 4, it is noted that the volumetric strain depicts a huge dilation in case of sample S1 (void ratio 0.58), whereas sample S3 (void ratio 0.73) depicts compressive behavior. Similar tendency is noticed in the experimental studies. It should be emphasized that the volumetric strain is increasing at 10% axial strain even though the stress ratio approaches to same value at this stage.

Figure 5 depicts the evolution of b value with ε_1 for different void ratios. Note that, b value increases gradually with ε_1 until it reaches a peak. The evolution of b has nice similarity to that of the stress ratio. The evolution of b depicts a unique characteristics at large strain for sample S2 and S3. The evolution of b for sample S3, on the other hand, depicts no unique behavior. However, it can be presumed that the unique characteristic might observe at a strain larger than 10% regardless of the void ratio of the numerical sample.

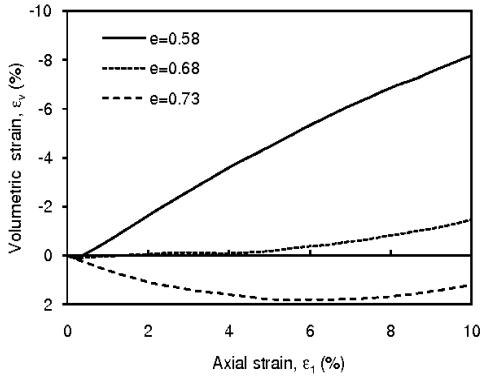

Figure 4: Relationship between volumetric strain ε_v and axial strain ε_1

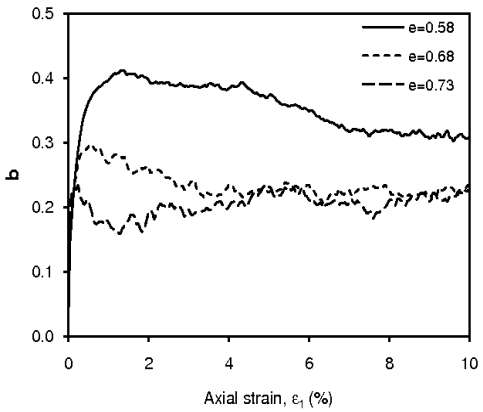

Figure 5: Evolution of b value with ε_1 for different void ratios of the sample

6.2 Micro-mechanical responses:

One of the objectives of this paper is to report the micro-behavior of granular materials evolve during the simulation in PSC. Figure 6 depicts the evolution of coordination number with ε_1 while Figure 7 depicts the evolution of sliding contact fraction in PSC for samples having different void ratios. Mathematically, coordination number and sliding contact fraction can be defined as follows:

$$C = \frac{2N_c}{N_p} \qquad (3)$$

$$S_r = \frac{N_s \times 100}{N_c} \qquad (4)$$

where N_c is the total number of contacts between particles, N_p is the total number of particles used in the simulation and N_s is the number of sliding contacts. Note that, both the coordination number and sliding contact fraction depict a unique behavior at the larger strain regardless of the void ratio of the numerical samples. This indicates that a critical state is reached for these micro-parameters at large strain.

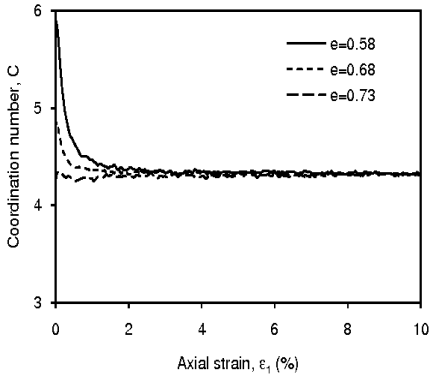

Figure 6: Evolution of coordination number C with axial strain ε_1

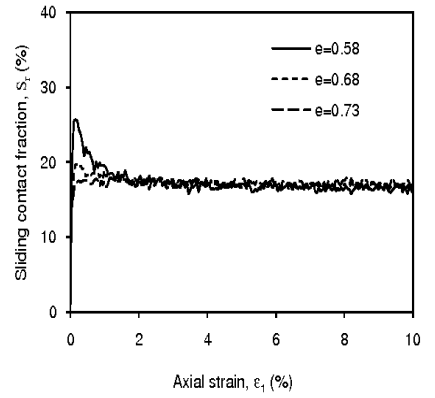

Figure 7: Evolution of sliding contact fraction S_r with axial strain ε_1

The evolution of contact fabric ratios H_{11}/H_{33} and H_{22}/H_{33} for all contact is depicted in Figure 8 while the evolution of contact fabric ratios H^s_{11}/H^s_{33} and H^s_{22}/H^s_{33} for strong contact is depicted in Figure 9. The contact fabric for all and strong contact is quantified using the following fabric tensors (Sazzad and Suzuki, 2012):

$$H_{ij} = \frac{1}{N_c}\sum_{c=1}^{N_c} n_i^c n_j^c \qquad (5)$$

$$H_{ij}^s = \frac{1}{N_c}\sum_{s=1}^{N_c^s} n_i^s n_j^s \qquad (6)$$

where, n_i^c and n_i^s is the components of unit normal vector at c -th contact and s -th strong contact, respectively. A contact is said to be a strong contact if it carries force greater than the average force. The average force is calculated as follows:

$$f_{ave} = \sqrt{\frac{\sum_{k=1}^{N_c}\left|f^k\right|^2}{N_c}} \qquad (7)$$

where f^k is the $k-$th force. The evolution of fabric ratios H_{11}/H_{33} and H_{22}/H_{33} for all contact does not truly represent the stress-strain behavior (see Figure 8), while the evolution of fabric ratios H^s_{11}/H^s_{33} and H^s_{22}/H^s_{33} for strong contact represents the stress-strain behavior vividly. This suggests a linkage between the stress ratio σ_1/σ_3 and fabric ratio H^s_{11}/H^s_{33} and between the stress ratio σ_2/σ_3 and fabric ratio H^s_{22}/H^s_{33} .

The relationships between the fabric ratio H^s_{11}/H^s_{33} and the stress ratio σ_1/σ_3 and between the fabric ratio H^s_{22}/H^s_{33} and the stress ratio σ_2/σ_3 are depicted in Figure 10. An excellent correlation between the fabric ratio and stress ratio is found. The relationship between them can be expression as follows:

$$\frac{H^s_{11}}{H^s_{33}} = 1.37\left(\frac{\sigma_1}{\sigma_3}\right) - 0.35 \qquad (8)$$

$$\frac{H^s_{22}}{H^s_{33}} = 1.33\left(\frac{\sigma_2}{\sigma_3}\right) - 0.31 \qquad (9)$$

From equations (8) and (9), one can infer than the linkage between the fabric measure and stress ratio can be described by almost a common relationship.

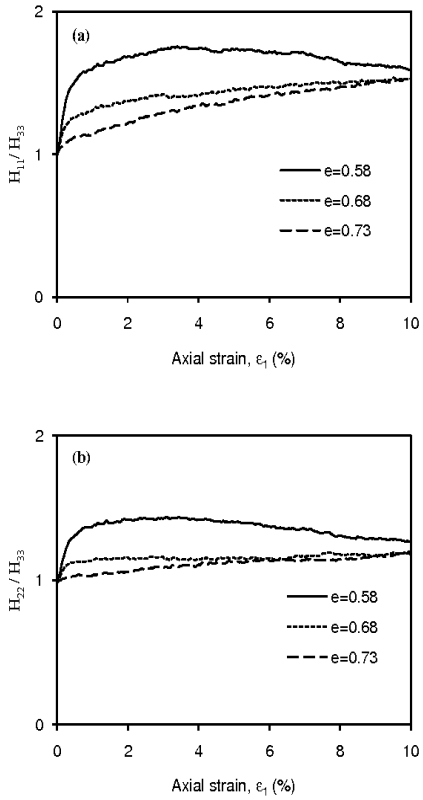

Figure 8: Evolution of (a) H_{11}/H_{33} with ε_1 and (b) H_{22}/H_{33} with ε_1

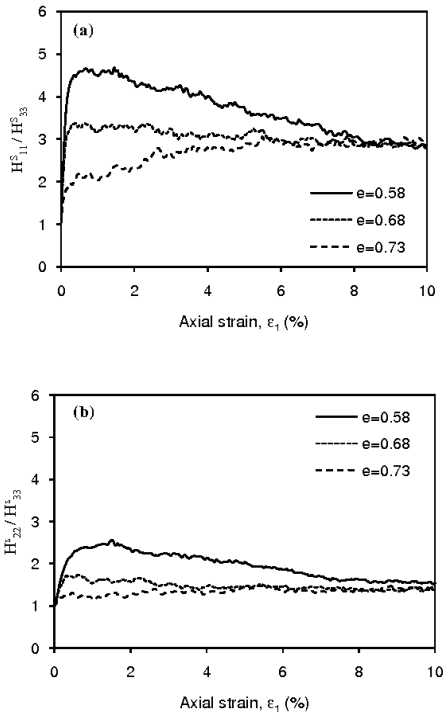

Figure 9: Evolution of (a) H^s_{11}/H^s_{33} with ε_1 and (b) H^s_{22}/H^s_{33} with ε_1

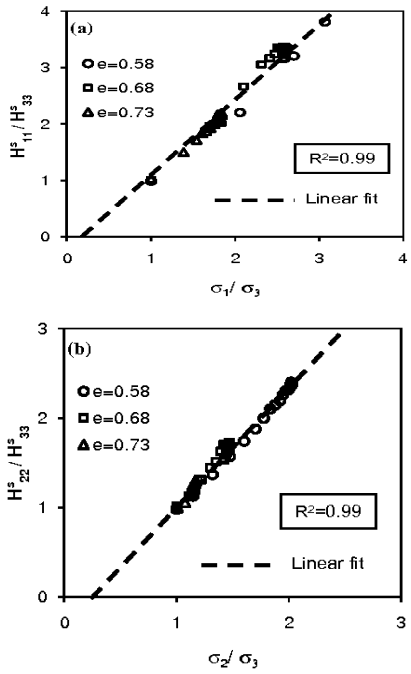

Figure 10: Relationships between (a) the fabric ratio H^s_{11}/H^s_{33} and the stress ratio σ_1/σ_3 and (b) the fabric ratio H^s_{22}/H^s_{33} and the stress ratio σ_2/σ_3

7. Conclusions:

Numerical simulation of PSC tests are conducted in the present study to investigate the macro and micro-mechanical behavior of granular materials such as sand under varying void ratio. Three cubical shaped numerical samples were prepared using spheres to carry out the PSC test. The simulated macro results are in good agreement with the experimental results, which ensures the qualitative validation and versatility of the current simulated results. The micro behaviors are also studied in details. Few important points of this study can be noted as follows:

i) The evolution of b value with axial strain has qualitative similarity with the evolution of stress ratio with axial strain and depicts uniqueness at large strain.

ii) Micro parameters such as the coordination number and sliding contact fraction reach the critical state at small strain level for PSC conditions.

iii) An excellent linkage between the contact fabric and stress ratio is established regardless of the void ratio of the numerical samples when only the strong contacts are considered.

iv) The linkage between the fabric measures and stress ratios can be described by a linear relationship for PSC.

References:

[1] Alshibli, K. A. and Asbas, I. S. (2007). "Strain localization in clay: plane strain versus triaxial loading conditions.", *Geotechical and Geological Engineering*, 25(1), 45–55.

[2] Alshibli, K. A., Batiste, S. N. and Sture, S. (2003). "Strain Localization in Sand: Plane Strain versus Triaxial Compression.", *Journal of Geotechnical and Geoenvironmental Engineering*, 129(6), 483-499.

[3] Cornforth, D. H. (1964). "Some experiments on the influence of strain conditions on the strength of sand", *Geotechnique*, 14(2), 143–167.

[4] Cundall, P. A. (1971). "A computer model for simulating progressive, large scale movements in blocky rock systems.", *In: Proceedings of the ISRM Symposium on Rock Fracture, Nancy,France, A. A. Balkama, Rotterdam*, Paper II-8, pp. 129–136.

[5] Cundall, P. A.,and Strack, O. D. L.(1979).**"**A discrete numerical model for granular assemblies**"**, *Geotechnique*, 29(1),47-65.

[6] Kuhn, M. R. (1999). "Structured deformation in granular materials.*", Mechanics of Materials*, 31(6), 407-429.

[7] Kuhn, M. R. (2005). **"**Are granular materials simple? An experimental study of strain gradient effects and localization**"**, *Mechanics of Materials*, 37(5), 607-627.

[8] Kuhn, M. R. (2006). **"**OVAL and OVALPLOT: Programs for analyzing dense particle assemblies with the discrete element method.", http://faculty.up.edu/kuhn/oval/doc/oval_0618.pdf., last access: April 10,2012.

[9] Lee, K. (1970). ''Comparison of plane strain and triaxial tests on sand.'', *J. Soil Mech. Found. Div.*, 96(3), 901–923.

[10] Ng, T. -T.(2004)." Macro-and micro-behaviors of granular materials under different sample preparation methods and stress paths", *International Journal of Solids and Structures;* 41(21), 5871-5884.

[11] Peters, J. F., Lade, P. V., and Bro, A. (1988). "Shear Band Formation in Triaxial and Plane Strain Tests", *Advanced Triaxial Testing of Soil and Rock*, ASTM STP977; Robert T. Donaghe, Ronald C., Chancy and Marshall L. Silver Eds., Philadelphia, 604-627.

[12] Sazzad, K., and Suzuki, K. (2012). "A comparison between conventional triaxial and plane-strain compression on a particulate system using 3D DEM." *Acta Geotechnica Slovenica, 9(2), 17-23.*

[13] Tatsuoka, F., Sakamoto, M., Kawamura, T. and Fukushima, S. (1986). ''Strength and deformation characteristics of sand in plane strain compression at extremely low pressures.'' *Soils and Foundation*, 26(1), 65–84.

[14] Tejchman, J. and Wu, W. (2010). "Boundary effects on behaviour of granular material during plane strain compression." *European Journal of Mechanics A/Solids*, 29(1), 18–27.

[15] Yasin, S. J. M. and Tatsuoka, F. (2006). "Stress-strain behavior of a micacious sand in plane strain condition.", *Soil Stress-Strain Behavior: Measurement, Modeling and Analysis, Geotechnical Symposium in Rome, "La Sapienza", Italy*, 16-